CALIBRATION AND ANALYSIS OF ORBITAL ACCURACY THROUGH SST OBSERVATIONS

Noelia Sánchez-Ortiz, Raúl Domínguez-González, Nuria Guijarro-López, and Jaime Nomen-Torres

Deimos Space, Ronda de Poniente 19, 28760, Tres Cantos, Madrid, 28760, Spain, Email: {noelia.sanchez, raul.dominguez, nuria.guijarro, jaime.nomen}@deimos-space.com

ABSTRACT

Current efforts on development and deployment of SST systems have resulted in an increasing number of sensors. Integration of those sensors into the SST systems normally requires an initial qualification step to ensure their correctness and robustness. This process, commonly known as calibration is commonly based on the sensors observing objects whose accurate reference orbits are publicly available. These orbits are considered the ground truth in this process. The evaluation of residuals of those observations with respect to the reference orbit provides information on the noise associated to the sensor measurements and the identification of any relevant bias. Biases can then be compensated for and the errors coming from the measurements bounded.

Once sensors are properly calibrated, their observations can also be considered as ground truth. In that case, orbital information (provided by SST services or made available by satellite operators) can be evaluated against this ground truth in order to provide an analysis of typical errors found in the orbital information (process called by the authors 'inverse calibration'). Deviation from the orbital information is caused by initial errors in the determination process generating the orbits but also due to the propagation from that initial state affected by the velocity errors, and the uncertainty of the perturbing models and object parameters.

TLE data is made publicly available, although its associated uncertainty is not provided. Several authors have provided methods to assess the typical accuracy of this data set. This paper describes the observed accuracy through this inverse calibration process for several objects and it also provides some statistical results. Observed deviations of TLE-based predictions from calibrated measurements reach from hundreds of meters up to kilometres, depending on the orbital regime, the propagation time span and the object itself.

In addition to the poor accuracy TLE catalogue, the more precise Special Perturbation (SP) catalogue is made available by 18th Space Control Squadron to some users. Like the TLE catalogue, the SP catalogue also lacks uncertainty information. This paper analyses also, through the inverse calibration process, the observed accuracy of the SP data sets for different orbital regimes. Deviations of SP orbits from tens to hundreds of meters have been observed with this method. Cases will be presented showing the performance of the method with accurate orbital predictions; TLE and SP are compared for the same objects.

Keywords: SSA; SST; Surveillance; Tracking; Calibration.

1. INTRODUCTION

Deimos Sky Survey (DeSS) is an optical observatory placed in Niefla mountains (Ciudad Real, Spain), located in a Natural Park with very dark skies, aimed to detect and track near-Earth space objects (NEAs) and Earth-orbiting objects (satellites and space debris). At the date of this document it comprises four different sensors that perform surveillance and tracking tasks (Figure 1). The control centre is located at Elecnor Deimos premises in Puertollano (Figure 1). A dedicated radio link is used to control the telescopes covering the 40 km distance.

The observatory is focused on GEO and MEO surveillance with three of the sensors performing that activity. The fourth dome has been used first for an experimental LEO sensor, that has evolved into the current sensor "Antsy" optimized for LEO. The approach for the LEO sensor is remarkably different to the GEO/MEO sensors, as the relative velocity of the LEO objects is much larger than GEO or MEO. This has a direct impact in the quality of the astrometry, and work has been put in place to mitigate the impact of this.

- **Time accuracy** A critical part of the obtention of the astrometry is to get accurate timestamps of the observations. It is necessary to consider not only the aspects of the observation itself, but also the delays involved in software execution or different hardware elements. In order to minimise the issues, dedicated software and hardware has been put in place with the objective of making the timestamp errors below ± 4 microseconds (with this, the error in the apparent

Figure 1. DeSS domes and control centre

position is in the order of magnitude of the observed satellite itself).

- **Exposure times and trailing losses** Observations are performed by exposing a Charge-coupled device (CCD) to the focused light. In case of moderately long exposure times, the photons from the observed object are spread on several pixels. Thus, the signal over each individual pixel is reduced, and the Signal-to-noise (SNR) ration is reduced accordingly. This effect is called trailing loss. We minimise the trailing loss by minimising the exposure time.

2. DESCRIPTION OF ANTSY TELESCOPE

The results presented in this paper were obtained from the Antsy sensor. Reference [1] provides a very detailed description of the sensor. Antsy uses a fork mount, this mount allows agile movement, which is very relevant for tracking LEO objects (fast movers, and following varying paths), avoiding the problems that can be found in other conventional equatorial mounts. It is mounted in a clamshell dome. The dome contains only the telescope and related hardware. As it is controlled remotely, it is not necessary to have room for a person inside the dome, thus the overall solution is extremely compact, as seen in Figure 2.

The optical assembly has a short focal length system with a very wide and fast focal relation. This is necessary for LEO tracking, because of the high angular speed of the target and the extremely short exposure times required (as mentioned before). In addition to this, there is a non-negligible uncertainty in the position of the tracked object when using Two-Line Elements TLE data for tracking. For example, [2] shows that it is not uncommon to find errors up to 10 km in the TLE-predicted position in LEO. As TLE-based tracking is very common, the sensor has a moderately wide field of view in order to compensate this.

Finally, the CCD is a frame transfer chip with a size of 1024x1024 pixels, covering a Field of View of 1.6º x 1.6º. This does not cover the corrected full field of view of the optical design, but is acceptable for the purpose of LEO. The choice of a frame transfer chip prevents all the timestamping problems found with mechanical and rolling electronic shutters, while the resolution of 1024x1024 allows to quickly download the information from the CCD (thus increasing the rate at which the sensor can obtain its measurements).

3. SP CATALOGUE DATA

The SP (Special Perturbation) catalogue is maintained by the 18th Space Control Squadron (18 SPCS) from the United States Space Force. This catalogue implements a detailed propagation theory, and is widely recognised as more precise than the General Perturbation (GP) catalogue (also known as TLE catalogue). The SP catalogue data is provided by 18 SPCS upon agreement ([3]). The orbits in the SP catalogue are obtained from the Space Surveillance Network (SSN), which is a world-wide network devoted to the space surveillance [4].

The SP catalogue includes ephemeris of the Earth-orbiting satellites covering a few days in the future. The ephemeris provided allow interpolation, thus, for obtain-
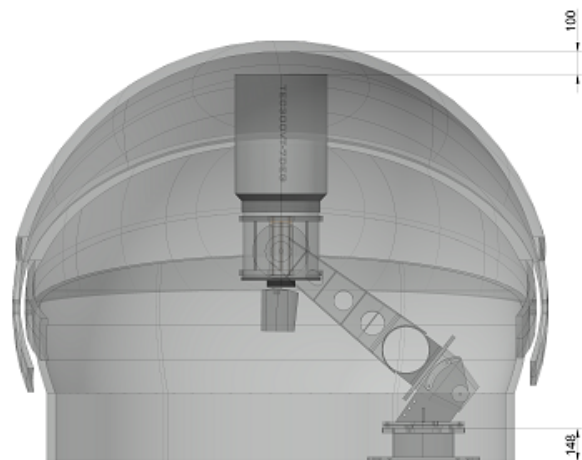

Figure 2. Antsy and dome schematic

ing the state vector of a satellite at a given point, it is enough to perform an interpolation on the given SP data. It is thus not necessary to propagate, and therefore, when interpolating, there is no loss of accuracy (that could happen in the case of propagating).

4.   CALIBRATION PROCEDURES

The design discussed above is the result of years of work. The way of discovering inaccuracies in the optical observations has always been the comparison of observed data against precise reference data. This work has been done during these years with the CALMA (CALibration Measurement Ancillary Tool) developed by Deimos Space. At its core, it computes the differences between the real measurements and a reference. Knowing these differences provides valuable insights while evaluating the performance of the optical sensor that is being calibrated. The differences are displayed to the user in the Right Ascension / Declination space. In addition to this, they are projected in an intrinsic reference frame bound to the satellite (Along-track, cross-track, radial, ACR). The following data can be used as reference:

- **SP3C format** Global Navigation Satellite Systems (GNSS) provide their ephemeris in this format. This is the prime reference, as the ephemeris for all the satellites in the GNSS constellations are routinely made public, reaching accuracies down to the centimeter level.

- **CPF format** CPF (Consolidated Prediction Format) data is routinely provided by the for laser ranging satellites routinely tracked by International Laser Ranging Service (ILRS). Laser ranging measurements are extremely accurate for a small subset of objects (those equipped with a retroreflector). Thus, they are a valuable reference.

- **OEM format** The Orbit Ephemeris Message (OEM) is a standard format maintained by the Consultative Committee for Space Data Systems CCSDS [6]. CALMA uses this to perform calibration against orbit data provided by individual providers.

- **TLE format** TLE format is supported as a reference data.

- **SP format** The SP catalogue data in the format provided by [3]

As part of the operational procedures at DeSS, routine calibrations of all the telescopes are performed every month using GNSS satellites as reference (as most of the sensors are devoted to MEO and GEO observations, using GNSS is a sensible choice). The CALMA tool is used to support these calibrations.

5.   LEO SENSOR CALIBRATION PROCEDURE

The sensor used for this paper is focused on LEO, therefore, we perform its calibration against ILRS objects in LEO. As the observations of LEO are subject to all the particularities summarised in section 1, a calibration of this sensor against non LEO objects would not display all the issues mentioned before. Here we present a summary of the calibration process, the full process is described at [1].

The calibration shown here was performed by tracking the Starlette satellite. This is a passive satellite launched by the CNES (Centre National d'Études Spatiales) devoted to geodetic and geophysical research. It is a sphere (24 cm diameter) covered with 60 laser retroreflectors, with the objective of enabling its routine observation with satellite laser ranging equipments. The satellite is routinely tracked by the ILRS and thus, there are available CPF files that can be used as a reference for CALMA. In the next figure (Figure 3) we present the residuals computed with the CALMA tool, projected into the ACR frame and translated into time bias.
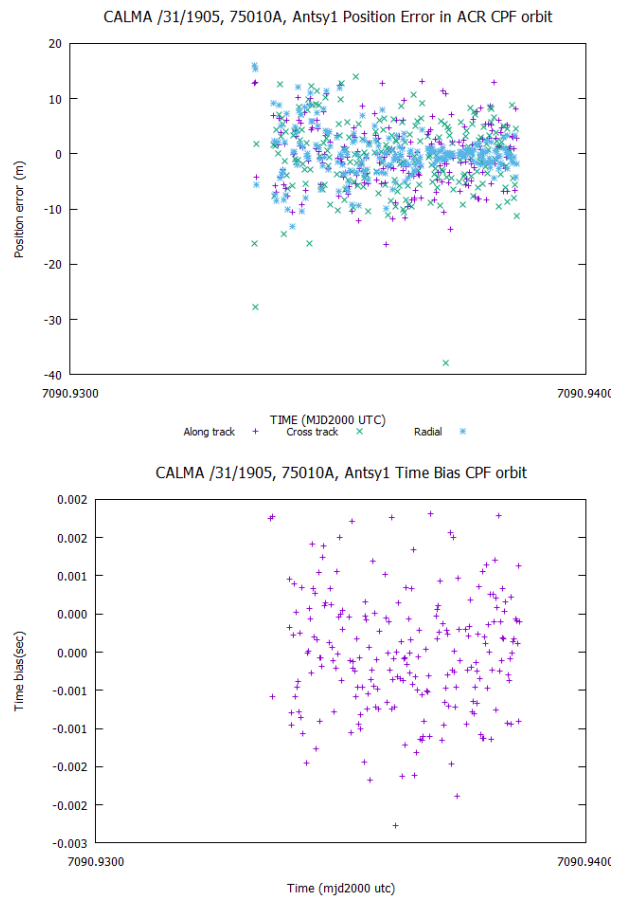

Figure 3. Example of calibration results (ACR residuals and time bias)

The first plot shows that the ACR residuals are evenly dispersed around zero. In particular, an along-track residual

with a zero average indicates that no time bias is present (an along-track bias translates directly into a time bias, as shown in the second plot). We also see that the distribution of cross-track and radial errors have similar dispersion values. Having the same dispersions for along-track and the other components indicates that the contribution of the time-tagging to the dispersion is negligible (this is, time bias has been completely removed). The overall width of the uncertainties in all the components is related the the determination of the centroid of the observation (and thus to the resolution of the system). Finally, the cross-track and along-track do not show any increasing or decrasing trend. This ensures that the sensor location has been determined with the adequate accuracy.
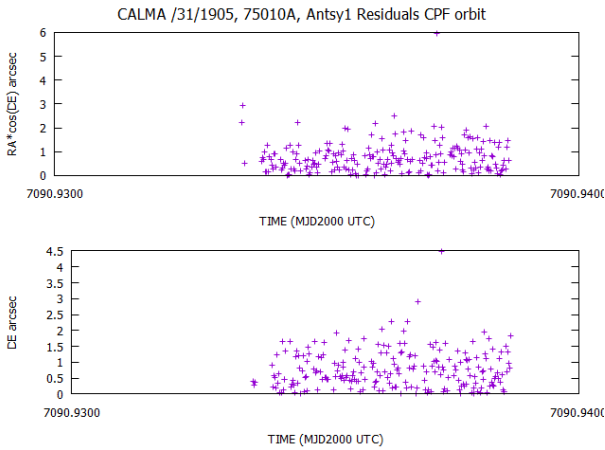

Figure 5. *Example of calibration results (Elevation profile)*

Name	COSPAR ID	Apogee/Perigee altitude (km)	Inclination (°)
JASON-3	2016-002A	1344-1332	66
JASON-1	2001-055A	1331-1320	66
DELTA 2 R/B	2008-012B	1200-196	39.8
WESTFORD	1963-014AK	3847-3410	87.3
WESTFORD	1963-014AU	4641-2447	86.8
WESTFORD	1963-014DM	3683-3608	87.4
WESTFORD	1963-014E	3691-3567	87.4
WESTFORD	1963-014EA	4477-2768	87.2
WESTFORD	1963-014EG	3723-3547	87.4
WESTFORD	1963-014H	3890-3391	87.3
WESTFORD	1963-014S	5706-1338	85.8
WESTFORD	1963-014X	4492-2731	85.8
SL-6 R/B(2)	1981-016E	35800-3850	68.2
BREEZE-M DEB	2016-005C	19378-365	49.4

Table 1. *Summary of objects analysed in this paper*

Figure 4. *Example of calibration results (Right ascension and declination residuals)*

Figure 4 presents the residuals in right ascension and declination. It can be seen that they are below 2 arcseconds and with no significant trends or artefacts visible. This is larger than the dispersion found in the other DeSS sensors (which stay below 1 arcsecond), and is related to the chosen arcseconds/pixel resolution for LEO.

The pass lasted just a few minutes (as it is a LEO pass). In Figure 5 we see that, during the pass, the elevations ranged from the potential minimum to the potential maximum. We see no features in Figures 3 and 4 associated with the extrema in Figure 5, this shows that the tracking motion is not affecting the quality of observations, and that effects related to low elevations are properly corrected.

6. LEO CAMPAIGN RESULTS

In this section, we present the result of an observation campaign that took place between 25th May 2019 to 2nd June 2019. During these nights, observations were scheduled on objects with perigee altitudes below 6000 km. Observations were scheduled based exclusively on opportunity (this is, 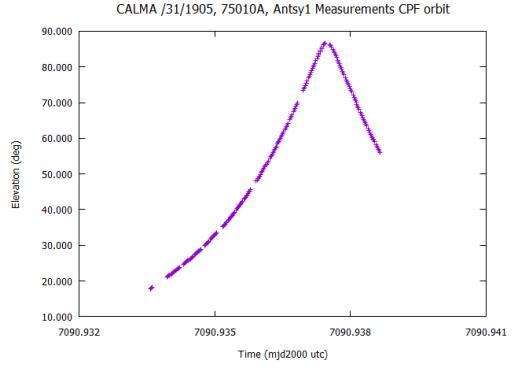if observations were feasible, they were tasked). This yielded a large amount of data on a variety of low objects (More than 500 tracks overall). For each of the passes, we made use of CALMA to compare the observations against the SP catalogue entry and the TLE catalogue entre. If we assume that the sensor is correctly calibrated (as shown in section 5), then CALMA can be used to assess independently the quality of the TLE and/or SP entries for individual objects. This is, if the sensor is calibrated correctly, all the differences seen in CALMA in these cases will be caused by the reference data, and thus we can obtain insights about the quality of the reference data. We call this process *inverse calibration*.

In general, we understand that the quality of the catalogue data will depend on the last time when an orbit determination has been done when the catalogue was produced, and the amount of data available at the time of that orbit determination. Thus, we can expect results ranging from very good accuracies (for objects that have been intensively tracked recently) to somewhat worse accuracies (for other objects). In the following subsections we present results from some objects deemed interesting. For all the objects (summarised in table 1), we present the ACR residual plots returned by CALMA, for SP and/or TLE catalogue references.

6.1. JASON-3

The first result we present here is for JASON-3. This satellite was among the observed in the campaign and, as there is ILRS data available for it, we take the advantage to double check our results using the precise ILRS reference. Figure 6 presents those results, proving that there are no apparent biases in the telescope data, and thus, it can be considered reliable.
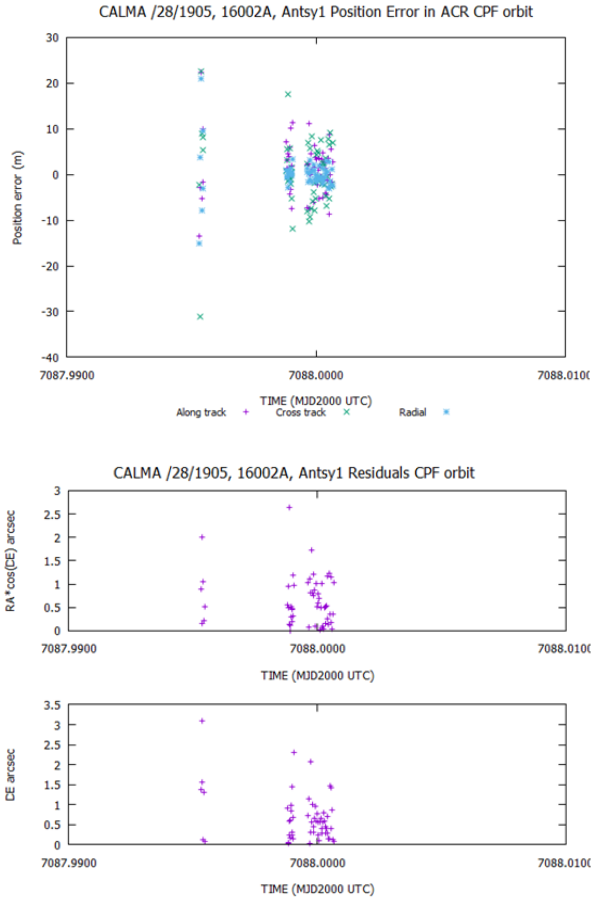

Figure 6. JASON-3 CALMA results against ILRS reference

Once we have determined the pass data is reliable, we proceed to compare the track against the SP and TLE catalogues data. Figure 7 presents those results. First, we see that, for both cases, we are misaligned with the reference data. In both cases, the residuals are dominant in the along-track direction. However, the residuals in the radial direction are of the same order of magnitude (even though they are a bit smaller). Also, we see that, for this case, the SP reference is one order of magnitude better than the TLE reference.

The residuals in the TLE plot show a defined behaviour, which is probably caused by the propagation theory that is being used. That behaviour is less apparent in the SP case, and only appreciable in the radial plane. Also, we see that, in both cases, the cross-track component is of similar order of magnitude. This implies that, in this case, both references approximate the orbital plane with similar accuracy.
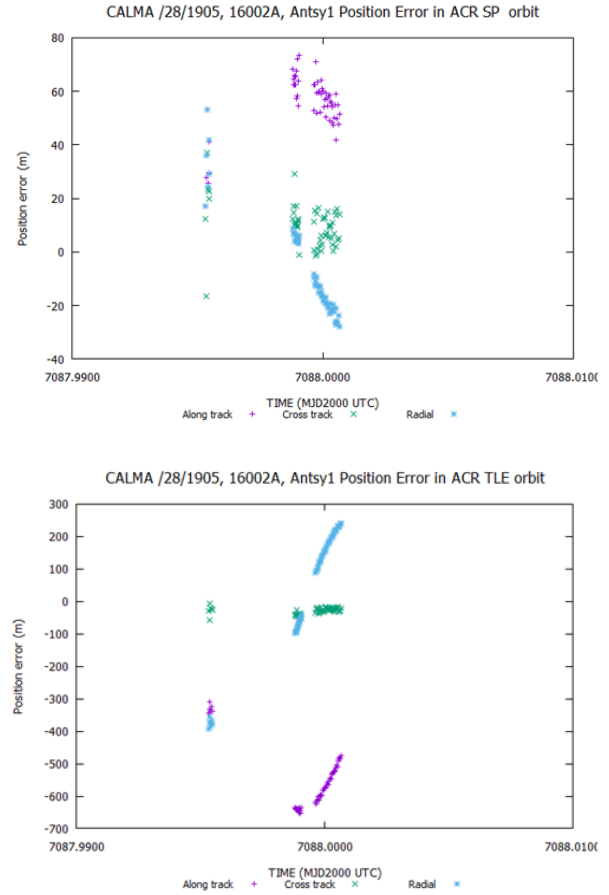

Figure 7. JASON-3 CALMA results against SP and TLE references

6.2. JASON-1

In this case, we consider JASON-1 which is in the same orbit as JASON-3, with observations taken the same night. We see in Figure 8 a similar order of magnitude for SP catalogue. In this case, the residuals in Along-track and radial are of the same order of magnitude. We also see that the cross-track component is properly centered around zero (thus, in this case, the orbital plane is correctly represented). In the TLE figure, we see a worse behaviour. Also, in this case, the cross-track component in the TLE picture is not centered in zero and shows a decreasing trend.

6.3. DELTA 2 R/B

This object with COSPAR ID 2008-012B was approaching re-entry at the date of the observations (the obser-
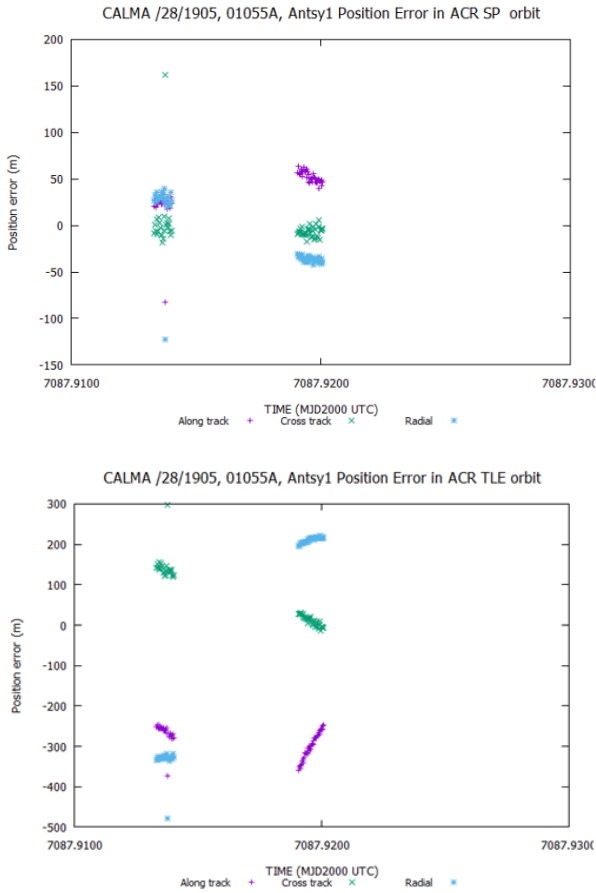
CALMA /28/1905, 01055A, Antsy1 Position Error in ACR SP orbit

CALMA /28/1905, 01055A, Antsy1 Position Error in ACR TLE orbit

Figure 8. JASON-1 CALMA results against SP and TLE references

CALMA /29/1905, 08012B, Antsy1 Position Error in ACR SP orbit

Figure 9. DELTA 2 R/B CALMA results against SP reference

COSPAR ID	Description	RCS (m^2)
1963-014AK	Dipoles	0.17
1963-014AU	Dipoles	0.22
1963-014DM	Dipoles	0.09
1963-014E	Midas solar array cover	0.4
1963-014EA	Cluster	0.31
1963-014EG	Dipoles	0.23
1963-014H	Package part	n/a
1963-014S	Dipoles	0.16
1963-014X	Dipoles	0.18

Table 2. Identification and RCS from observed West Ford objects

vations were taken in May/June 2019, and it is listed to have re-entered at the end of August). As it was nearing re-entry, its orbit was being severely affected by the atmospheric drag, affecting the reachable accuracy. In this case, as was a large object, the brightness was favourable. In Figure 9 we see that, for this case, the catalogue prediction was deviated by 80 kilometers. The radial component is also highly deviated. With such large deviations, the along-track and radial components are coupled (inaccuracies in radial component translate in along-track inaccuracies shortly after). We also see very large deviations in the cross-track component. This component usually behaves very well (the orbit of the plane is well determined). Therefore, we assume that the orbit determination solution for this re-entering case did probably not have enough data to provide a more accurate solution.

6.4. WEST FORD

The West Ford project released $4.8 \cdot 10^8$ copper dipoles, each 0.00178 cm in diameter and 1.78 cm in length in May 1963. They were released into a near-circular polar orbit at a mean altitude of 3650 km [7]. Most of the needles have re-e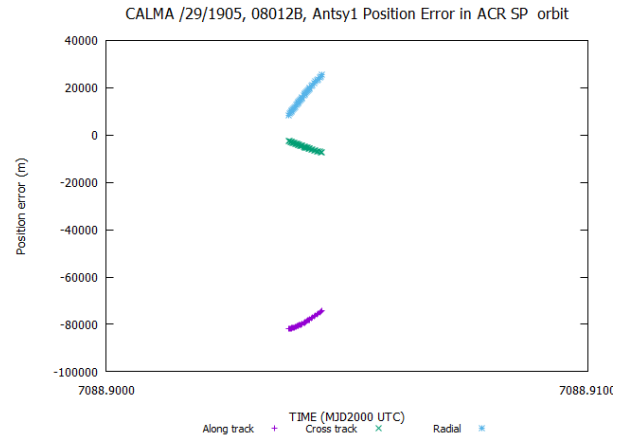ntered because of the long-term perturbations that increased their eccentricity until re-entry. However, there are still some objects associated to this experiment in orbit. These include dispensers and other mission-related objects, and also clumps of needles that failed to separate. These objects were deployed in roughly the same orbit as the needles themselves, but they are less affected by the perturbations (because of their lower Area-to-mass ratio). Table 2 lists the objects that were observed, together with their identification and Radar-cross-section (RCS). The data in this table was obtained from [8].

In Figures 10 and 11 we present the results for several different West Ford objects. The first result we can present is a very large variability in the accuracies, that range from meters to up to 8 kilometers. The presence of some cases in which we see a very good accuracy (1963-014DM and 1963-014E) shows that the optical telescope is able to produce correct accuracy. It also shows that the catalogue data for these objects can reach a large accuracy (we assume its actual accuracy will depend on the amount of data available at the time of determining the orbit, as discussed above). It is also worth noting that there is no apparent relationship between the radar cross section and the accuracy. All the objects listed here have similar radar cross section values, so the relationship between these is probably too weak to be observed here.

Another interesting feature we can observe is that the accuracy of SP and TLE results is coupled for all the cases. This is hardly surprising, as we assume that both solutions are generated from basically the same data. The results we present here provide a solid support for that assumption. We also see that, for this case, the accuracy of the SP and TLE catalogues is comparable (they are of the same order of magnitude in both cases). Case 1963-014S is particularly striking, because it shows a better accuracy for the TLE data than for the corresponding SP data. Again, we assume the orbits were obtained by different processes, so it is not surprising to find some cases in which the TLE solution fits better with the data, even though in general the SP model yields better solutions because of its more detailed underlying physical model.
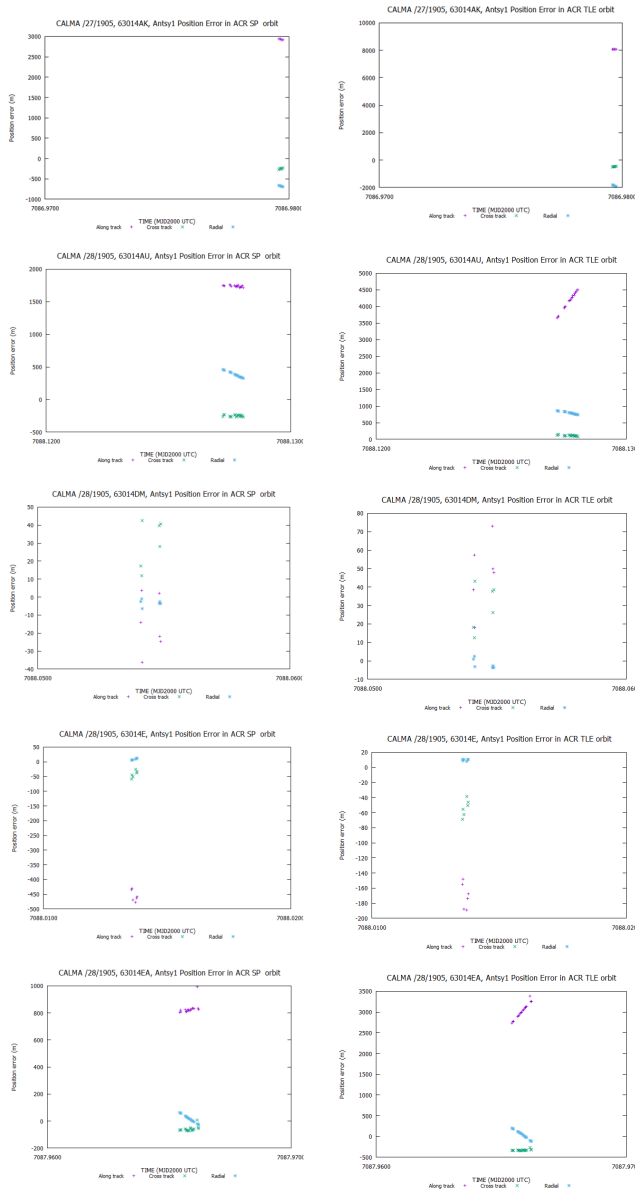

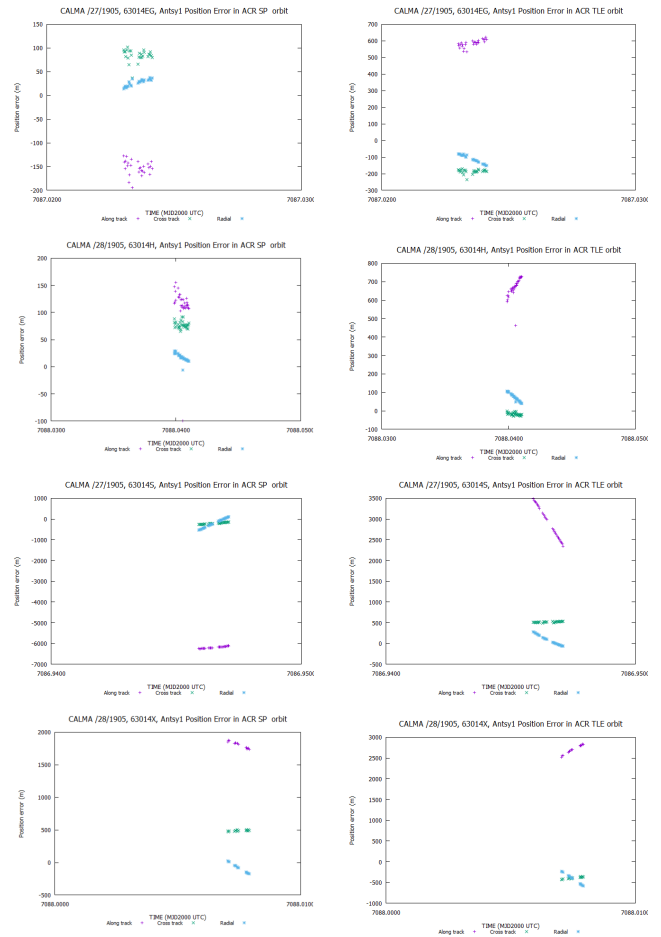Figure 11. *Several West Ford cases (left column: SP, right column: TLE)*

6.5. SL-6 R/B(2)

This case is a highly eccentric orbit, with its perigee at 3850 km altitude. This puts it well outside the LEO region, and makes it an interesting case. As the satellite is not affected at all by the atmospheric drag (unlike other eccentric objects or LEO), we expect the SP solution to be good (as the object is subject to well-modelled forces only). Figure 12 shows that the orbit in the SP catalogue is quite good, with just an along-track deviation of 100 meters and zero-centered cross track and radial differences.. As this object was in an orbit outside the regions of interest for conjunction assessment, it is reasonable to assume that the SSN does not perform dedicated tracking on it. Thus, we see that even with non dedicated tracking, the SSN is able to produce good quality orbits in this MEO regime. The TLE result is worse by an order of magnitude in all the components, but it is still a good result, that is more than enough to ensure that the object can be tracked and maintained in the catalogues.

In addition to this plot, we provide Table 3 with the accuracies reached for similar objects (eccentric orbits with apogee outside the Earth atmosphere). We see a very
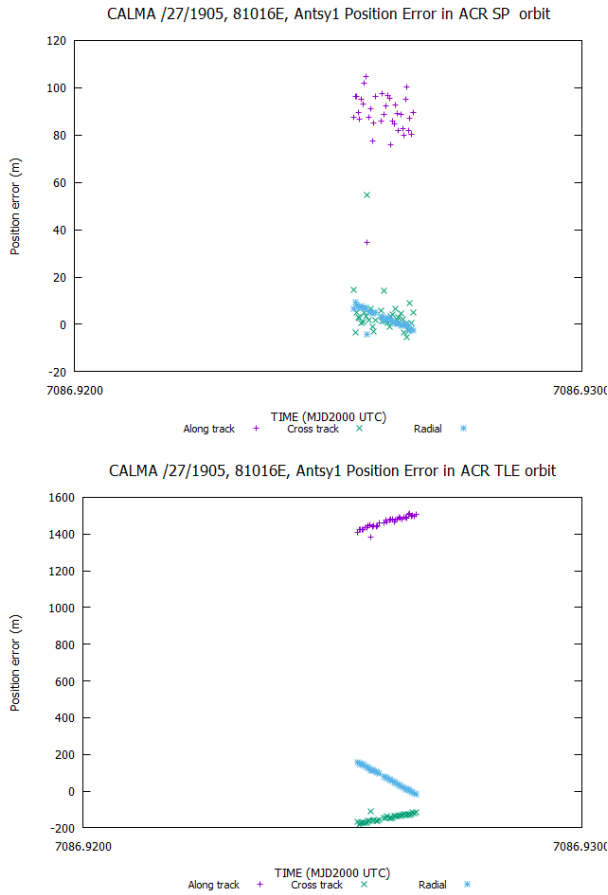

Figure 10. *Several West Ford cases (left column: SP, right column: TLE)*

Figure 12. *SL-6 R/B(2) CALMA results against SP and TLE references*

good result for the 1997-022D (another rocket body), and much worse results for the two others, which are debris from a fragmentation.

6.6.   BREEZE-M DEB [TANK]

This case is a highly eccentric orbit, with its perigee well into the Earth atmosphere. This makes it different from the cases in section 6.5. In this case, each perigee pass means a pass inside the Earth atmosphere, which results in a tiny decrease of the energy of the orbit and thus its apogee. The change in apogee in turn results in a change in the orbit period. For this reason, this regime is more vulnerable to errors in the orbit determination (i.e,

COSPAR ID	SP Average residual (m)	TLE Average residual (m)
1981-031D	1300	-1100
1981-031G	-620	3000
1997-022D	8	1600

Table 3. *Average along-track residuals for several eccentric cases*

tiny differences between the real and the estimated orbit quickly grow because of the constant change of the orbit period). In addition to this, the pass through the atmosphere adds the contribution of the drag force, which is modelled but with a certain degree of uncertainty.
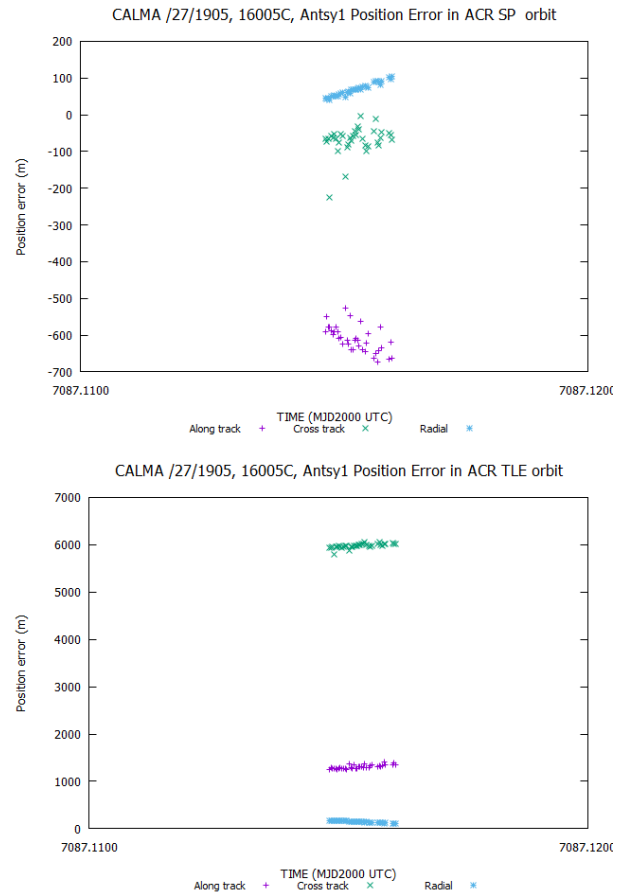

Figure 13. *BREEZE-M DEB [TANK] CALMA results against SP and TLE references*

In Figure 13 we see that for this relatively large object, we get residuals in along-track component of around 600 meters. We can also see a general trend in the radial difference with large values. This means that the difference between the estimated and the real orbits for this object grow steadily after the date of the track we are analysing.

Table 4 presents results for similar objects (eccentric with their perigee inside the Earth atmosphere). We have added the RCS, obtained from [9]. We see no strong relation between the reported RCS and the accuracy for the small number of cases shown here. Indeed, the best result is obtained for the object with the smallest reported RCS, this suggests that cross section is not the most relevant source of uncertainty in these cases.

Case 2010-007G shows an average of zero in the TLE case, but this is a limitation of the comparison, as the radial component for that same case has a 2000 m difference. Also it is worth noting that case 2009-075C shows an SP result much worse than the TLE. Even though in

COSPAR ID	Name	RCS	SP	TLE
1985-118L	SL-12 R/B(AUX MOTOR)	0.62	300	-1700
1989-001G	SL-12 R/B(AUX MOTOR)	0.62	-380	-1500
2008-044B	BREEZE-M DEB [TANK]	5	-125	3600
2009-016C	BREEZE-M DEB [TANK]	6.3	-700	550
2009-075C	BREEZE-M DEB [TANK]	7	-2100	-350
2010-007G	SL-12 R/B(AUX MOTOR)	0.6	-40	0*
1964-038A	ELEKTRON 3	-1100	2.8	-210
1969-009A	ISIS 1	2.1	-25	-700

Table 4. Average along-track residuals (m) for several eccentric cases

general SP behaves better than TLE, it is clear that this does not happen always.

7. CONCLUSIONS AND FUTURE WORKS

This analysis has shown that good quality observations of LEO objects are obtainable from the Antsy telescope. The method we have presented here (inverse calibration) allows us to evaluate the quality of the orbit data provided by the SSA catalogue providers, and could be trivially expanded for evaluating orbits determined by satellite operators. This quality assessment is very simple and straightforward, and it can be done without performing any orbit determination procedure. The primary input data (observed tracks) can be used as well in orbit determination.

The inverse calibration method needs software applying all relevant corrections, as well as extremely well-calibrated hardware in order to be successful. In the case of LEO objects, it is necessary to make use of telescopes designed specifically for the particularities of the LEO regime: quick and agile mounts, relatively large field of view and extremely quick download times.

We have shown that it is possible to use the optical measurements to quickly assess the validity of previously known solutions in case of re-entering objects. Of course, the astrometry data can be used as well in the orbit determination process of re-entering objects.

In future works we expect to:

- Expand the analysis to GEO regime.

- Provide statistical results of the accuracy of the different catalogues by aggregating and tabulating all the data.

- Make use of this concept for quick manoeuvre confirmation. As the process we are performing is extremely sensitive, tiny deviations (such as those after a manoeuvre) can be identified immediately, without requiring any orbit determination procedure.

REFERENCES

1. Noelia Sánchez-Ortiz, Jaime Nomen Torres, Raúl Domínguez-González, Nuria Guijarro, Daniel Lubián Arenillas *Operational observations of LEO objects with optical sensors: Extended observational campaigns* International Astronautical Congress, 2019

2. Raul Domínguez-González, Noelia Sánchez-Ortiz, Holger Krag, Johannes Gelhaus *Analysis of uncertainties of catalogued orbital data for the update of the ESA DRAMA ARES tool*, International Astronautical Congress, 2012

3. https://space-track.org *SP data source* Data used in agreement with 18SPCS ODR 19-061-2B

4. *NASA Spacecraft Conjunction Assessmentand Collision Avoidance Best Practices Handbook*, 2020

5. https://ilrs.gsfc.nasa.gov/ *International Laser Ranging Service*

6. https://public.ccsds.org/Pubs/502x0b2c1e2.pdf *Orbit Data Message*

7. I.I. Shapiro, H.M. Jones, C.W. Perkins *Orbital properties of the West Ford dipole belt* DOI:10.1109/PROC.1964.2992

8. McDowell, Jonathan C. *General Catalog of Artificial Space Objects, Release 1.1.9* , https://planet4589.org/space/gcat (2021)

9. Celestrak website https://www.celestrak.com